
Article:
Ilin, Konstantin orcid.org/0000-0003-2770-3489, Moffatt, H.K. and Vladimirov, Vladimir (2017) Dynamics of a rolling robot. Proceedings of the National Academy of Sciences of the United States of America. pp. 12858-12863. ISSN 1091-6490

https://doi.org/10.1073/pnas.1713685114

Dynamics of a Rolling Robot

K.I.Ilin [*], **H. K. Moffatt** [†], **and V.A.Vladimirov** [‡] [*]

[*]Department of Mathematics, University of York, Heslington, York,YO10 5DD, UK,[†]Department of Applied Mathematics and Theoretical Physics, University of Cambridge, Wilberforce Road, Cambridge CB3 0WA, UK, and [‡]Department of Mathematics and Statistics, Sultan Qaboos University, Oman.

Submitted to Proceedings of the National Academy of Sciences of the United States of America

Equations describing the rolling of a spherical ball on a horizontal surface are obtained, the motion being activated by an internal rotor driven by a battery mechanism. The rotor is modelled as a point mass mounted inside a spherical shell, and caused to move in a prescribed circular orbit relative to the shell. The system is described in terms of four independent dimensionless parameters. The equations governing the angular momentum of the ball relative to the point of contact with the plane constitute a six-dimensional, non-holonomic, non-autonomous dynamical system with cubic nonlinearity. This system is decoupled from a subsidiary system that describes the trajectories of the center of the ball. Numerical integration of these equations for prescribed values of the parameters and initial conditions reveals a tendency towards chaotic behaviour as the radius of the circular orbit of the point mass increases (other parameters being held constant). It is further shown that there is a range of values of the initial angular velocity of the shell for which chaotic trajectories are realised while contact between the shell and the plane is maintained. The predicted behaviour has been observed in our experiments.

non-holonomic system | internal rotor | chaotic rolling | rolling robot

Significance Statement

The dynamics of a rolling ball activated by an internal battery mechanism is analysed by theoretical and numerical techniques. The problem involves four independent dimensionless parameters, and is governed by a six-dimensional non-holonomic non-autonomous dynamical system with cubic nonlinearity. It can serve as a prototype for rolling bodies activated by any internal mechanism, and is relevant to robotic systems for which such internal mechanism may be subject to remote control. This is believed to be the first problem of its kind to have been solved by appeal to fundamental principles of classical dynamics. For this reason, it should be accessible to a wide readership. The numerical results provide clear evidence of both regular and chaotic behaviour.

Introduction

An intriguing toy, known as the 'Beaver Ball', consists of a rigid hollow sphere, inside which is mounted an eccentric battery-driven rotor. When this ball is placed on the floor with the rotor activated, it rolls in an apparently chaotic manner, a behaviour designed to appeal to kittens and mathematicians alike (typical behaviour may be seen in videos in the supplemental material to this paper). The beaver-ball phenomenon invites the following analysis, which is relevant to a class of problems involving robots with internal mechanisms that can in principle be remotely controlled; indeed the beaver ball may be considered as a simple prototype of such systems. We shall find that, despite the apparent simplicity of the structure of the toy, it admits a wide range of behaviour dependent on four governing dimensionless parameters and showing sensitive dependence on initial conditions characteristic of chaotic behaviour.

A general procedure for problems of this type involving non-holonomic constraints was described in the seminal paper of Chaplygin (1897) [1] (see also Neimark & Fufaev 2004 [2]). Application of this procedure for particular problems is however exceedingly complex, and we have found it preferable, and physically more revealing for the present problem, to return to first principles, starting simply with linear and angular momentum equations relative to a fixed frame of reference. When these equations are transformed to a suitably defined body frame of reference, a very helpful decoupling of equations determining the angular velocity of the spherical shell and its instantaneous orientation becomes apparent. This decoupling is exploited in the subsequent numerical investigation.

Idealised model

Consider a rigid uniform spherical shell of mass M and radius a. Suppose that a thin straight rod is mounted within the shell, coinciding with a diameter AB, and on bearings at A and B that allow free rotation of the rod about its axis (see figure 1). Let D be a point on AB at distance $d\,(<a)$ from the centre O' of the sphere. Suppose that a second rod DP of length b is rigidly fixed at D perpendicular to AB (with $b^2+d^2<a^2$ so that P lies inside the sphere), and that a point mass m is fixed at P. The mass of the rods is assumed negligible compared with either M or m, so the total mass of the ball is just $M+m$. An internal battery mechanism is such that the rod structure APB may be made to rotate about AB with constant angular velocity σ. The ball is placed on a plane horizontal surface, on which it is free to roll without slipping under the influence of gravity g. The problem is then to determine its motion.

We note that this is an over-simplification of the structure of the actual toy beaver ball, since the intrinsic rotational energy of the rotor also contributes to the dynamics. It seems reasonable however, in the interest

Reserved for Publication Footnotes

of simplicity, to adopt the above idealised model. The relevant dimensionless parameters are

$$\mu = m/M, \quad \gamma = g/\sigma^2 a, \quad \beta = b/a, \quad \delta = d/a, \qquad [1]$$

with $\beta^2 + \delta^2 < 1$. Note that $\gamma^{1/2} \equiv n/\sigma$ where $n \equiv (g/a)^{1/2}$ is a natural 'gravitational frequency'.

Kinematic description

Let O be a point fixed in space in the horizontal plane containing the centre O' of the sphere. Let $Oxyz$ (with Oz vertically upwards, so $\mathbf{g} = (0, 0, -g)$), and $O'x'y'z'$ be Cartesian frames of reference fixed in space and in the body respectively; and let $O'xyz$ be a moving frame with origin at O' and axes permanently parallel to the axes of $Oxyz$. We may suppose that $O'z'$ is parallel to $O'A$, and that O and O' coincide at time $t = 0$. Let $\mathbf{X} = \overrightarrow{OO'} = (X(t), Y(t), 0)$ with $\mathbf{X}(0) = \mathbf{0}$. The motion of the spherical shell is determined by its angular velocity[1] $\mathbf{\Omega}(t)$ and the velocity $\mathbf{V}(t) = \dot{\mathbf{X}}$ of its centre O'. The point of contact C of the sphere with the plane is the vector $\mathbf{a}$ with components $(0, 0, -a)$ in the frame $O'xyz$.

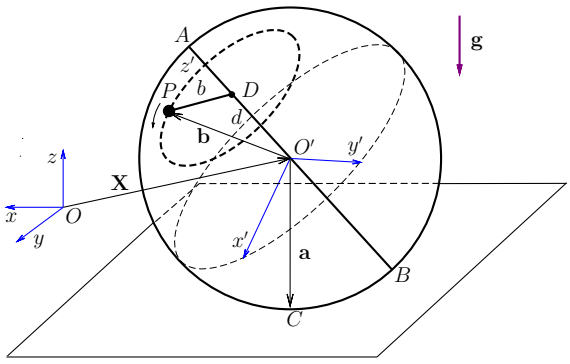

Fig. 1. Configuration sketch: the spherical shell rolls on a horizontal plane; the rod AB is on bearings at A and B that allow it to rotate freely about its axis; the rod DP is rigidly fixed at D at right angles to AB; a point mass m is fixed at P, and the rod structure APB is driven by a battery mechanism to rotate about AB with constant angular velocity σ; the axes $O'x'y'z'$ are fixed in the spherical shell.

The orientation of the sphere at any time may be described in terms of Euler angles $\{\theta, \phi, \psi\}$, defined (in the 'y-convention' of e.g., Goldstein, Poole & Safko 2002 [3], p. 601) as follows: starting with $O'x'y'z'$ in coincidence with $O'xyz$ and $O'A$ vertical (i.e. aligned with $O'z'$), rotate $O'x'y'z'$ through an angle ϕ about $O'z$, then through θ about $O'y'$, then through ψ about $O'z'$. Then the point $\mathbf{x}$ in $O'xyz$ is the same as the point $\mathbf{x}'$ in $O'x'y'z'$, where

$$\mathbf{x}' = \mathsf{A}\,\mathbf{x}, \qquad [2]$$

and where, with the compact notation $c_\theta \equiv \cos\theta, s_\theta \equiv \sin\theta$, etc., the orthogonal transformation matrix A is given by

$$\mathsf{A} = \begin{bmatrix} -s_\phi s_\psi + c_\theta c_\phi c_\psi & c_\phi s_\psi + c_\theta s_\phi c_\psi & -s_\theta c_\psi \\ -s_\phi c_\psi - c_\theta c_\phi s_\psi & c_\phi c_\psi - c_\theta s_\phi s_\psi & s_\theta s_\psi \\ s_\theta c_\phi & s_\theta s_\phi & c_\theta \end{bmatrix}. \qquad [3]$$

The inverse of A is its transpose A^T, and $\det \mathsf{A} = +1$.

For any vector $\mathbf{h}$ with components in $O'xyz$, we use the notation $\mathbf{h}' = \mathsf{A}\,\mathbf{h}$ for the same vector with components in the body frame $O'x'y'z'$. Thus, for example, with

$$\mathbf{\Omega} = \left(-\dot\theta\, s_\phi + \dot\psi\, s_\theta c_\phi,\ \dot\theta\, c_\phi + \dot\psi\, s_\theta s_\phi,\ \dot\phi + \dot\psi\, c_\theta\right), \qquad [4]$$

the components of $\mathbf{\Omega}' = \mathsf{A}\,\mathbf{\Omega}$ in $O'x'y'z'$ are, as may be verified,

$$\mathbf{\Omega}' = \left(\dot\theta\, s_\psi - \dot\phi\, s_\theta c_\psi,\ \dot\theta\, c_\psi + \dot\phi\, s_\theta s_\psi,\ \dot\phi\, c_\theta + \dot\psi\right). \qquad [5]$$

Similarly, with $\mathbf{a} = (0, 0, -a)$,

$$\mathbf{a}' = \mathsf{A}\,\mathbf{a} = a(\sin\theta\cos\psi,\ -\sin\theta\sin\psi,\ -\cos\theta). \qquad [6]$$

In the body frame $O'x'y'z'$, the point A has coordinates $(0, 0, a)$, and the mass m moves in the circular orbit

$$\mathbf{b}'(t) = \overrightarrow{O'P} = (b\cos\sigma t,\ b\sin\sigma t,\ d) \qquad [7]$$

(and then $\mathbf{b} = \mathsf{A}^\mathsf{T}\mathbf{b}'$). The important thing here is that $\mathbf{b}'(t)$ is a *prescribed* function of time. The method that follows can be used for any other prescription of $\mathbf{b}'(t)$, and can be generalised to any number of masses $\{m_1, m_2, m_3, \ldots\}$ with prescribed trajectories in $O'x'y'z'$, $\{\mathbf{b}'_1(t), \mathbf{b}'_2(t), \mathbf{b}'_3(t) \ldots\}$.

Now the position vector of the mass m in the frame $Oxyz$ is given by $\mathbf{x}_m = \mathbf{X} + \mathbf{b}$, and its velocity in this frame is

$$\mathbf{v}_m = \dot{\mathbf{X}} + \dot{\mathbf{b}} = \mathbf{V} + \mathbf{v}, \quad \text{say.} \qquad [8]$$

Relative to the body frame $O'x'y'z'$, the velocity of m is

$$\mathbf{v}'_m = \mathbf{V}' + \mathbf{v}' = D\mathbf{X}' + D\mathbf{b}', \qquad [9]$$

where the operator D is defined for any vector $\mathbf{h}'(t)$ by

$$D\mathbf{h}' \equiv \dot{\mathbf{h}}' + \mathbf{\Omega}' \times \mathbf{h}',$$

and the dot represents time-differentiation. In particular, $\dot{\mathbf{\Omega}} = \dot{\mathbf{\Omega}}'$. Note further that, since $\mathbf{a} = (0, 0, -a)$ is constant,

$$\dot{\mathbf{a}} \equiv \dot{\mathbf{a}}' + \mathbf{\Omega}' \times \mathbf{a}' = 0, \qquad [10]$$

with the obvious first integral $|\mathbf{a}'|^2 = \text{cst}$. Finally, note that

$$D\mathbf{b}' = \dot{\mathbf{b}}' + \mathbf{\Omega}' \times \mathbf{b}', \qquad [11]$$

$$D^2\mathbf{b}' = \ddot{\mathbf{b}}' + \mathbf{\Omega}' \times (\mathbf{\Omega}' \times \mathbf{b}') + 2\mathbf{\Omega}' \times \dot{\mathbf{b}}' + \dot{\mathbf{\Omega}}' \times \mathbf{b}'. \qquad [12]$$

Here, $\mathbf{\Omega}' \times (\mathbf{\Omega}' \times \mathbf{b}')$ is the centrifugal acceleration and $2\mathbf{\Omega}' \times \dot{\mathbf{b}}'$ the Coriolis acceleration. The term $\dot{\mathbf{\Omega}}' \times \mathbf{b}'$ is

[1] The list (1) of dimensionless parameters may be supplemented by the parameter Ω_0/σ, where $\Omega_0 = |\mathbf{\Omega}(0)|$ is determined by initial conditions.

known as the Poincaré acceleration in astronomical contexts.

Rolling and contact conditions

The rolling condition (a non-holonomic constraint) expresses the fact that the point C of the spherical shell is instantaneously at rest for all t, i.e.

$$\mathbf{V} + \mathbf{\Omega} \times \mathbf{a} = 0 \quad \text{and so also} \quad \dot{\mathbf{V}} = \mathbf{a} \times \dot{\mathbf{\Omega}}\,. \qquad [13]$$

The forces acting on the ball are its weight $(M+m)\mathbf{g}$ and the force $\mathbf{F} = (F_x,\, F_y,\, F_z)$ at the point of contact C. The frictional contribution $(F_x,\, F_y,\, 0)$ serves simply to maintain the rolling conditions [13]. The normal contribution $(0,\, 0,\, F_z)$ prevents vertical motion of the centre O', and we must require that $F_z > 0$ for all t to ensure permanent contact with the plane. Since the maximum upward force on the ball due to the rotation of the mass m is of order $mb\,\sigma^2$, we may expect that contact will be maintained provided $(M+m)g \gtrsim mb\,\sigma^2$, or in terms of the dimensionless parameters [1], provided

$$(1+\mu)\gamma \gtrsim \mu\,\beta. \qquad [14]$$

This condition will be refined in [35] below.

Equations of motion

We consider now the equations for the rate of change of the linear momentum of the system,

$$\mathbf{p} = M\,\mathbf{V} + m\,\mathbf{v}_m, \qquad [15]$$

and of its angular momentum relative to the point O,

$$\begin{aligned} \mathbf{L} &= \mathbf{X} \times M\,\mathbf{V} + (\mathbf{X}+\mathbf{b}) \times m\,\mathbf{v}_m + I\,\mathbf{\Omega} \\ &= \mathbf{X} \times \mathbf{p} + m\,\mathbf{b} \times \mathbf{v}_m + I\,\mathbf{\Omega}\,, \end{aligned} \qquad [16]$$

where I is the moment of inertia of the shell. These equations are

$$\dot{\mathbf{p}} = (M+m)\mathbf{g} + \mathbf{F}\,, \qquad [17]$$

and

$$\dot{\mathbf{L}} = \mathbf{X} \times M\mathbf{g} + (\mathbf{X}+\mathbf{b}) \times m\mathbf{g} + (\mathbf{X}+\mathbf{a}) \times \mathbf{F}. \qquad [18]$$

Using [16] and [17], [18] can be written in the form

$$I\,\dot{\mathbf{\Omega}} + m\mathbf{b} \times \dot{\mathbf{v}}_m = m\mathbf{b} \times \mathbf{g} + \mathbf{a} \times \mathbf{F}\,. \qquad [19]$$

Eliminating $\mathbf{F}$ from [17] and [19], and using [15], we obtain

$$I\,\dot{\mathbf{\Omega}} - M\,\mathbf{a} \times \dot{\mathbf{V}} + m\,\mathbf{s} \times \dot{\mathbf{v}}_m = m\,\mathbf{b} \times \mathbf{g}\,, \qquad [20]$$

where $\mathbf{s} = \mathbf{b} - \mathbf{a}$. Now we eliminate $\mathbf{V}$ from [20] using the rolling conditions [13] and $\mathbf{v}_m = \mathbf{V} + \mathbf{v}$. After simplification, this gives

$$I\,\dot{\mathbf{\Omega}} - M\,\mathbf{a} \times (\mathbf{a} \times \dot{\mathbf{\Omega}}) + m\,\mathbf{s} \times (\mathbf{a} \times \dot{\mathbf{\Omega}}) + m\,\mathbf{s} \times \dot{\mathbf{v}} = m\,\mathbf{b} \times \mathbf{g}\,. \qquad [21]$$

This equation describes the rate of change of angular momentum of the ball relative to the point C of the shell, which is instantaneously at rest.

So far, we have expressed these dynamical equations in the rest frame $Oxyz$. However, since the motion of the point P in the body frame $O'x'y'z'$ is known, it makes sense to rewrite [21] relative to the body frame. As this is a vector equation, it holds equally in the body frame, with $\mathbf{a}$ replaced by $\mathbf{a}'$ and similarly for the other vectors in the equation. Using the fact that $\mathbf{g} = n^2\mathbf{a}$, the plane being horizontal, the transformed equation is

$$\begin{aligned} I\,\dot{\mathbf{\Omega}}' - M\,\mathbf{a}' \times \left(\mathbf{a}' \times \dot{\mathbf{\Omega}}'\right) + m\,\mathbf{s}' \times \left(\mathbf{a}' \times \dot{\mathbf{\Omega}}'\right) \\ +\; m\,\mathbf{s}' \times D^2\mathbf{b}' = m\,n^2\,\mathbf{b}' \times \mathbf{a}'. \end{aligned} \qquad [22]$$

Noting [12], and bringing all the terms involving $\dot{\mathbf{\Omega}}'$ to the left, this equation takes the form

$$\begin{aligned} m^{-1}\mathsf{Q}\,\dot{\mathbf{\Omega}}' \;=\; & -\mathbf{s}' \times \ddot{\mathbf{b}}' - 2\mathbf{s}' \times \left(\mathbf{\Omega}' \times \dot{\mathbf{b}}'\right) \\ & -\left(\mathbf{b}' \cdot \mathbf{\Omega}'\right)\left(\mathbf{s}' \times \mathbf{\Omega}'\right) + \left(n^2 + \mathbf{\Omega}'^2\right)\mathbf{b}' \times \mathbf{a}', \end{aligned} \qquad [23]$$

where Q is the symmetric matrix with elements

$$Q_{ik} = \left(I + Ma^2 + m\mathbf{s}'^2\right)\delta_{ik} - Ma'_i a'_k - ms'_i s'_k. \qquad [24]$$

Note that Q is positive definite, given that $I > 0$. When coupled with [10], i.e. with

$$\dot{\mathbf{a}}' + \mathbf{\Omega}' \times \mathbf{a}' = 0\,, \qquad [25]$$

eqns. [23] – [25] constitute a six-dimensional, non-autonomous, non-holonomic dynamical system, with cubic nonlinearity[2], for the components of $\mathbf{a}'(t)$ and $\mathbf{\Omega}'(t)$, having the obvious first integral $\mathbf{a}'^2 = a^2 = \text{cst}$. It is noteworthy that this system is decoupled from eqn. [5], which in principle determines the evolution of the Euler angles $\{\theta(t), \phi(t), \psi(t)\}$, once $\mathbf{\Omega}'(t)$ is known. We do not however need to determine these Euler angles, which is fortunate because if θ approaches zero, the angles ϕ and ψ become indeterminate.

Non-dimensionalisation

From this point on, we take $I = \frac{2}{3}Ma^2$, the value for a thin spherical shell, so $I + Ma^2 = \frac{5}{3}Ma^2$. With dimensionless variables defined by[3]

$$\tau = \sigma\,t,\;\; \hat{\mathbf{\Omega}} = \mathbf{\Omega}'/\sigma,\;\; \hat{\mathbf{a}} = \mathbf{a}'/a,\;\; \hat{\mathbf{b}} = \mathbf{b}'/a,\;\; \hat{\mathbf{s}} = \hat{\mathbf{b}} - \hat{\mathbf{a}}, \qquad [26]$$

eqns. [23]–[25] take the form

$$\begin{aligned} \mu^{-1}\hat{\mathsf{Q}}\,\hat{\mathbf{\Omega}}_\tau \;=\; & -\hat{\mathbf{s}} \times \hat{\mathbf{b}}_{\tau\tau} - 2\hat{\mathbf{s}} \times \left(\hat{\mathbf{\Omega}} \times \hat{\mathbf{b}}_\tau\right) \\ & -\left(\hat{\mathbf{b}} \cdot \hat{\mathbf{\Omega}}\right)\left(\hat{\mathbf{s}} \times \hat{\mathbf{\Omega}}\right) + \left(\gamma + \hat{\mathbf{\Omega}}^2\right)\hat{\mathbf{b}} \times \hat{\mathbf{a}}, \end{aligned} \qquad [27]$$

$$\hat{\mathbf{a}}_\tau \;=\; \hat{\mathbf{a}} \times \hat{\mathbf{\Omega}}, \qquad [28]$$

where now $\hat{\mathsf{Q}}$ is the matrix with elements

$$\hat{Q}_{ik} = \left(\tfrac{5}{3} + \mu\,\hat{\mathbf{s}}^2\right)\delta_{ik} - \hat{a}_i\hat{a}_k - \mu\,\hat{s}_i\hat{s}_k, \qquad [29]$$

and where, from [7], the orbit of the mass m is now prescribed as

$$\hat{\mathbf{b}} = (\beta\cos\tau, \beta\sin\tau, \delta). \qquad [30]$$

As expected, eqns. [27]–[30] contain the four dimensionless parameters μ, γ, β and δ defined by [1].

[2] This cubic nonlinearity is evident, e.g. in the term $\mathbf{\Omega}'^2\mathbf{b}' \times \mathbf{a}'$ of [23] in which $\mathbf{b}'(\tau)$ is prescribed.
[3] Alternatively, we may define $\tilde{\mathbf{\Omega}} = \mathbf{\Omega}'/n = \gamma^{-1/2}\hat{\mathbf{\Omega}}$, with corresponding adjustments in [27] and [28].

The trajectory $\mathbf{X}(\tau)$ of the ball

In order to determine the trajectory $\mathbf{X}(\tau)$ of the ball, it is not enough to solve [27] and [28]: we also need to integrate the rolling condition $\dot{\mathbf{X}} = \mathbf{a} \times \boldsymbol{\Omega}$. We may again bypass the Euler angles as follows. Let $\mathbf{e}_1$ and $\mathbf{e}_2$ be unit vectors along the coordinate axes $O'x$ and $O'y$. Then $\mathbf{e}_1'$ and $\mathbf{e}_2'$ (the same vectors relative to the rotating axes) satisfy the equations

$$\mathbf{e}_{1\tau}' = \mathbf{e}_1' \times \hat{\boldsymbol{\Omega}}\,, \quad \mathbf{e}_{2\tau}' = \mathbf{e}_2' \times \hat{\boldsymbol{\Omega}}\,. \qquad [31]$$

Having solved these, $X(\tau)$ and $Y(\tau)$ (non-dimensionalised with a) are determined by integration of the components of [13]; noting that the scalar product of any two vectors is frame-independent, these give

$$X_\tau = \sigma^{-1}\boldsymbol{\Omega}\cdot\mathbf{e}_2 = \hat{\boldsymbol{\Omega}}\cdot\mathbf{e}_2'\,,\ Y_\tau = -\sigma^{-1}\boldsymbol{\Omega}\cdot\mathbf{e}_1 = -\hat{\boldsymbol{\Omega}}\cdot\mathbf{e}_1'\,, \quad [32]$$

and, with the right-hand sides now known, direct numerical integration is straightforward.

The precise contact condition

With $\mathbf{V}\cdot\mathbf{e}_3 = 0$, and $\mathbf{v}_m\cdot\mathbf{e}_3 = \mathbf{v}\cdot\mathbf{e}_3$, where $\mathbf{e}_3 = (0,0,1)$, the vertical component of [17] gives

$$F_z = (M+m)g + m\frac{d}{dt}(\mathbf{v}\cdot\mathbf{e}_3) = (M+m)g + m\frac{d}{dt}(\mathbf{v}'\cdot\mathbf{e}_3'), \qquad [33]$$

using again the invariance of the scalar product. Now, with $\mathbf{v}' = D\mathbf{b}'$ and $\dot{\mathbf{e}}_3' = \mathbf{e}_3' \times \boldsymbol{\Omega}'$, we have

$$\frac{d}{dt}(\mathbf{v}'\cdot\mathbf{e}_3') = \mathbf{e}_3'\cdot\left[\frac{d}{dt}(D\mathbf{b}') + \boldsymbol{\Omega}'\times D\mathbf{b}'\right] = \mathbf{e}_3'\cdot D^2\mathbf{b}'\,, \qquad [34]$$

where $D^2\mathbf{b}'$ is given by [12]. Contact between the sphere and the plane is maintained provided $F_z > 0$. Hence, in dimensionless terms, with $\mathbf{e}_3' = -\hat{\mathbf{a}}$, this contact condition becomes

$$(1+\mu)\gamma > \mu\hat{\mathbf{a}}\cdot D^2\mathbf{b}', \qquad [35]$$

a condition that is satisfied provided γ is large enough; just how large it must be can be determined when $\hat{\mathbf{a}}(t)$ and $\hat{\boldsymbol{\Omega}}(t)$ are known, i.e. after [27] and [28] have been solved. The criterion [35] provides the required refinement of [14].

Particular cases

(i) Axisymmetric ball. If $\beta = 0$ in [30], the mass m is fixed on the diameter AB, and the ball is axisymmetric about this diameter. This is a well-known integrable case (Chaplygin 1897).

(ii) One-dimensional time-periodic solutions when $\delta = 0$. In this case D coincides with O' and the rod DP rotates in a diametral plane, and it is clear that there must exist time-periodic solutions for which the rod AB remains horizontal and the ball rolls in the y-direction perpendicular to AB. For this type of solution,

$$\hat{\boldsymbol{\Omega}}(\tau) = (0,0,\hat{\Omega}_3(\tau)) \quad \text{and} \quad \hat{\mathbf{a}}(\tau) = (\hat{a}_1(\tau), \hat{a}_2(\tau), 0),$$

and [27] and [28] simplify to

$$\left(\tfrac{5}{3} + \mu\,\hat{\mathbf{s}}^2\right)\hat{\Omega}_{3\tau} = -\mu\beta\,(\hat{a}_1\sin\tau - \hat{a}_2\cos\tau)\left(\gamma + (1+\hat{\Omega}_3)^2\right),$$
$$\hat{a}_{1\tau} = \hat{\Omega}_3\hat{a}_2, \quad \hat{a}_{2\tau} = -\hat{\Omega}_3\hat{a}_1, \qquad [36]$$

a three-dimensional dynamical system with periodic coefficients. In general this cannot be solved analytically; there are however two exact solutions given by

$$\hat{\Omega}_3(\tau) = -1, \quad \hat{a}_1 = \pm\cos\tau, \quad \hat{a}_2 = \pm\sin\tau, \qquad [37]$$

which correspond to steady rolling of the ball, with P either vertically below or above O' ($\pm$ signs in [37] respectively). The former solution is presumably stable, the latter unstable. For these solutions, the mass m is at rest relative to the centre of the shell, its rotation relative to the shell being exactly compensated by reverse rolling of the shell with the same frequency σ.

More generally, numerical solution of [36] using MATLAB shows that although the trajectory of the ball is a straight line, its velocity oscillates with time as the mass m rises and falls. Figure 2 shows the function $\Omega_3(\tau)$, which, starting very near the unstable solution, quickly become a periodic functions of τ, although (like an unstable compound pendulum) remaining for some time during each cycle in a close neighbourhood of the unstable configuration.

(iii) Solutions with $\beta \neq 0, \delta \neq 0$. In this more general situation, as may be verified, equations [27]-[30] still admit two particular solutions for which

$$\hat{\boldsymbol{\Omega}}(\tau) = (0,0,-1), \qquad \hat{\mathbf{a}}(\tau) = \pm\,\hat{\mathbf{b}}(\tau)/|\hat{\mathbf{b}}(\tau)|\,. \qquad [38]$$

For these solutions, the mass m is again at rest on the vertical line passing through the centre of the shell, either below the centre (stable) or above it (unstable), corresponding respectively to the $\pm$ in [38]. In either situation, the rolling of the ball is synchronous with the rotation of the rotor in just such a way that the mass m remains stationary, exerting zero moment about C. The corresponding trajectories [32] are straight lines.

Further numerical results

The following results were obtained by numerical solution of [27], [28], again using MATLAB. Writing [30] in the form

$$\hat{\mathbf{b}} = \rho(\tilde{\beta}\cos\tau, \tilde{\beta}\sin\tau, \tilde{\delta}), \qquad [39]$$

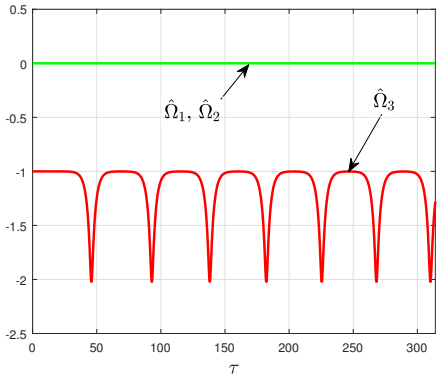

Fig. 2. Components of $\hat{\boldsymbol{\Omega}}$ vs. τ from numerical solution of [36], with $\mu = 1$, $\gamma = 1$, $\delta = 0$, $\beta = 1/2$, and with initial conditions $\hat{\boldsymbol{\Omega}}(0) = (0,0,-1)$, $\hat{\mathbf{a}}(0) = (-1,0,0)$.

where

$$\rho = |\hat{\mathbf{b}}| = \sqrt{\beta^2 + \delta^2}, \quad \tilde{\beta} = \beta/\rho, \quad \tilde{\delta} = \delta/\rho, \qquad [40]$$

we now prescribe the motion of the mass m inside the shell in terms of ρ and $\tilde{\beta}$; ρ is the constant (dimensionless) distance $O'P$ of m from the centre of the sphere, and is fixed at $\rho = \frac{1}{2}$ in the computations that follow.

The initial value of $\hat{\mathbf{a}}$ is given in terms of the Euler angles $\{\theta_0, \phi_0, \psi_0\}$ at time $\tau = 0$ from [6], i.e.

$$\hat{\mathbf{a}}(0) = (\sin\theta_0 \cos\psi_0, -\sin\theta_0 \sin\psi_0, -\cos\theta_0), \qquad [41]$$

(and ϕ_0 can be chosen to be zero). It is supposed that the mass m moves according to [39] for $\tau \geqslant 0$. In figures 3–7, the trajectories $(\hat{X}(\tau), \hat{Y}(\tau))$ start at $(0,0)$ (shown by a green circle) at time $\tau = 0$; they are computed for $0 < \tau < 300\pi$, i.e. for 150 periods of the motion of the mass m relative to the shell, the final point at $\tau = 300\pi$ being shown by a red asterisk.

The Lyapunov exponent λ was also computed for each trajectory, in order to detect sensitive dependence on initial conditions, and possible chaos. For this purpose, we used the MATLAB code of **?**[4], which computes the Lyapunov spectrum using the algorithm of **?**[5]. In all examples studied here, we found that $\hat{\mathbf{\Omega}}(\tau)$ was confined to a finite region of $\mathbb{R}^3$ containing the origin; since $\hat{\mathbf{a}}(\tau)$ is restricted to the unit sphere $|\hat{\mathbf{a}}| = 1$, the system therefore evolves in a finite region of $\mathbb{R}^6$. In this situation, the occurrence of a positive Lyapunov exponent indicates chaotic behaviour.

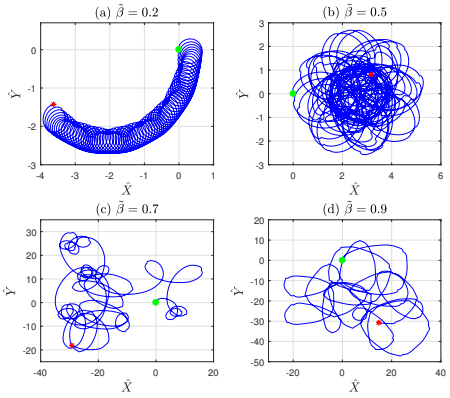

Fig. 3. Trajectories $\mathbf{X}(\tau)$ of the ball centre for $\mu = 1$, $\gamma = 1$, $\rho = 1/2$, $\tilde{\beta}$ as shown, and $\tilde{\delta}$ given by [40]; initial conditions [41] and [42]. Lyapunov exponents: (a) $\lambda \approx 0.002$; (b) $\lambda \approx 0.003$; (c) $\lambda \approx 0.053$; (d) $\lambda \approx 0.077$.

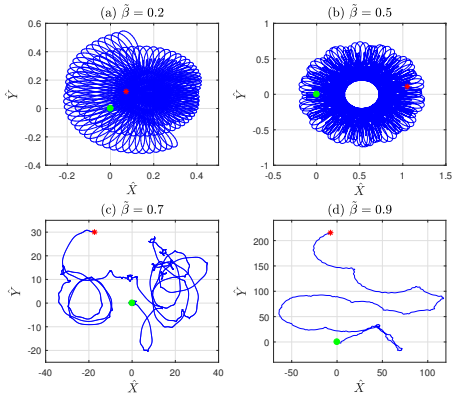

Fig. 4. Same as Fig.3, but with initial conditions given by [41] and [**??**]; (a) $\lambda \approx 0.002$; (b) $\lambda \approx 0.003$; (c) $\lambda \approx 0.102$; (d) $\lambda \approx 0.059$.

(i) Trajectory of the ball from a state of rest with mass m in lowest position.

Consider first the situation where the shell is initially at rest and the mass m is at its lowest position:

$$\hat{\mathbf{\Omega}}(0) = 0, \quad \psi_0 = 0, \quad \text{and} \quad \theta_0 = \arccos(-\tilde{\delta}). \qquad [42]$$

The computed trajectories $\{\hat{X}(\tau), \hat{Y}(\tau)\}$ are shown in figure 3. The Lyapunov exponents λ in the figure caption are positive, but close to zero for cases (a, b), and much

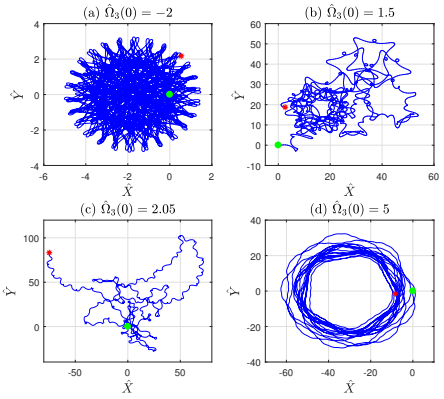

Fig. 5. Trajectories $\mathbf{X}(\tau)$ for $\mu = 2$, $\gamma = 4$, $\tilde{\beta} = 0.9$, $\tilde{\delta} \approx 0.436$; $\hat{\mathbf{a}}(0)$ given by [41]; $\hat{\mathbf{\Omega}}(0) = (0, 0, \hat{\Omega}_3(0))$, with $\hat{\Omega}_3(0)$ as indicated; Lyapunov exponents: (a) $\lambda \approx 0.004$; (b) $\lambda \approx 0.084$; (c) $\lambda \approx 0.093$; (d) $\lambda \approx 0.006$.

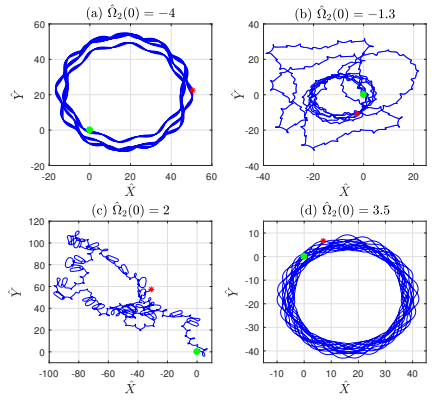

Fig. 6. Same as Fig.5, but with $\hat{\mathbf{\Omega}}(0) = (0, \hat{\Omega}_2(0), -1)$, $\hat{\Omega}_2(0)$ as indicated; (a) $\lambda \approx 0.005$; (b) $\lambda \approx 0.033$; (c) $\lambda \approx 0.103$; (d) $\lambda \approx 0.005$.

[4] The first two panels of Figures 3 and 4 suggest the possible existence of invariant tori for small β (i.e. near to the integrable case $\beta = 0$); there is perhaps lurking here a non-holonomic counterpart of the KAM theorem for near-integrable Hamiltonian systems, a proposition that certainly deserves detailed investigation. We are grateful to a referee for this interesting suggestion.

larger for (c, d), consistent with the apparent chaotic character of the latter trajectories.

(ii) Trajectory of the ball from a state of rest m in highest position.

For this case, the initial conditions are

$$\hat{\boldsymbol{\Omega}}(0) = 0, \quad \psi_0 = \pi, \quad \text{and} \quad \theta_0 = \arccos(-\tilde{\delta}), \qquad [43]$$

and corresponding trajectories are shown in figure 4. Again, the relatively large positive values of λ in the panels (c, d) are consistent with the apparent chaos of the trajectories.[4]

(iii) Effect of nonzero $\boldsymbol{\Omega}(0)$ *(and* $\mathbf{V}(0)$ *given by* [13]).

Figure 5 shows the results with initial angular velocity $\hat{\boldsymbol{\Omega}}(0) = (0, 0, \hat{\Omega}_3(0))$ for four different values of $\hat{\Omega}_3(0)$. In this case, λ is relatively large in panels (b) and (c), consistent again with the apparently chaotic trajectories. In the limiting situation $\hat{\Omega}_3(0) = -1$, the trajectory is a straight line along the y-axis corresponding to the exact solution [38]. Note here that not all values for $\hat{\Omega}_3(0)$ lead to solutions defined for all $\tau > 0$, because the contact condition [35] may fail for some $\tau = \tau_* > 0$. The computations show that [35] does actually hold at least up to $\tau = 300\pi$ provided $-5.96 \leq \hat{\Omega}_3(0) \leq 5.00$ (and fails just outside these limits).

If $\hat{\Omega}_3(0)$ is close to -1, the trajectory is close to a circle. As $|\hat{\Omega}_3(0)+1|$ increases from zero, the behaviour becomes more interesting, as evident in figure 5, but when $\hat{\Omega}_3(0)$ approaches either end of the interval $[-5.96, 5.00]$, the motion becomes more regular, e.g. near the left end, the trajectory is almost circular. This is because the effect of the mass m is small when the initial angular velocity magnitude $|\hat{\boldsymbol{\Omega}}(0)|$ is relatively large.

Figure 6 shows the behaviour with initial angular velocity $\hat{\boldsymbol{\Omega}}(0) = (0, \Omega_2(0), -1)$ for four values of $\Omega_2(0)$. Again, the contact condition [35] may fail for some $\tau = \tau_* > 0$; computation shows that, in this case, [35] holds up to $\tau = 300\pi$ provided that $|\hat{\Omega}_2(0)| \leq 5.55$ (and again fails for $|\hat{\Omega}_2(0)|$ just outside this limit). As $|\hat{\Omega}_2(0)|$ increases from zero, the behaviour of the ball rapidly becomes more complicated and there is a range of chaotic behaviour, before the orbit again settles down to nearly circular form as the value 5.55 is approached.

(iv) Behaviour for $\mu = 4.6, \gamma = 3.2, \beta = 0.5, \delta = 0$.

These parameter values (satisfying [14] by a good margin) are close to the actual values for the toy beaver ball. The left panel of figure 7 shows a random trajectory starting with $\boldsymbol{\Omega}(0) = 0$ near the unstable orientation (as indicated above the panel), and the right panel shows oscillations about a circular path starting near the stable orientation; note the difference of scale on the $\hat{X}$ and $\hat{Y}$ axes, also the large difference of scale between the two panels. The structure of the beaver ball is such that it is not possible to control the starting orientation of the internal rotor, but in repeated trials we have observed both types of behaviour — see the supplemental material for videos shot in the anti-chapel of Trinity College, Cambridge (videos best opened with *QuickTime Player*).

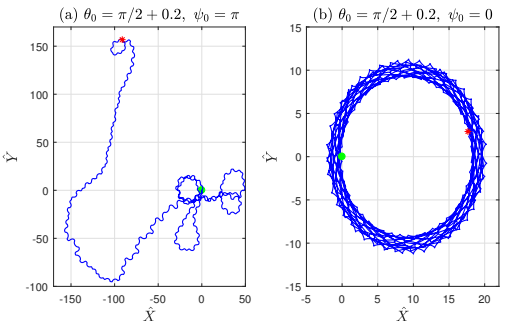

Fig. 7. Computed trajectories for parameter values $\mu = 4.6, \gamma = 3.2, \beta = 0.5, \delta = 0$; (a) trajectory starting with m near highest position, showing random behaviour at least up to $\tau = 300\pi$; (b) trajectory starting with m near lowest position, following a nearly circular path with oscillations of frequency σ. Note the difference of scale between the two panels.

Conclusions

We believe that this is the first theoretical and numerical study of a dynamical system that is both non-holonomic and driven by a specified internal mechanism, here a rotor on a prescribed orbit internal to a supporting spherical shell. The model may serve as a prototype for more complex robotic systems that are likewise subject to non-holonomic constraints.

The present simple 'Beaver Ball' model evolves in a six-dimensional phase space, in which a rich behaviour is to be expected. We have identified chaotic behaviour for various choices of the parameters, and for various initial conditions compatible with maintaining contact between the ball and the supporting plane. These results are presented in figures 2–6, while figure 7 shows the behaviour for parameter values representative of the actual toy beaver ball.

References

1 Chaplygin, S. A. (1897). On a motion of a heavy body of revolution on a horizontal plane. English translation: *Regular and chaotic dynamics* **7**(2) (2002), 119 –130.

2 Neimark, Ju. I. & Fufaev, N. A. (2004). *Dynamics of non-holonomic systems. Translations of Mathematical Monographs*, **33**, Amer. Math. Soc.

3 Goldstein, H., Poole, C. P. & Safko, J. L. (2002). *Classical Mechanics, 3rd Edn.* AAPT.

4 Govorukhin, V. N. (2004). `https://uk.mathworks.com/matlabcentral/fileexchange/4628-calculation-lyapunov-exponents-for-ode`

5 Wolf, A., Swift, J. B., Swinney, H. L. & Vastano, J. A. (1985). Determining Lyapunov exponents from a time series. *Physica D: Nonlin. Phen.*, **16**(3), 285–317.

ACKNOWLEDGMENTS. VAV acknowledges partial support from grant IG/SCI/DOMS/16/13 from Sultan Qaboos University, Oman. We thank three referees for their valued comments.